

# Extensive Study of the Wobbling Properties in $^{163}\text{Lu}$ for the Positive and Negative Parity States

Robert Poenaru <sup>\*1,2</sup> and Apolodor Aristotel Raduta <sup>†2,3</sup>

<sup>1</sup>Doctoral School of Physics, University of Bucharest, Romania

<sup>2</sup>*Horia Hulubei* National Institute for Physics and Nuclear Engineering,  
Măgurele-Bucharest, Romania

<sup>3</sup>Academy of Romanian Scientists, Bucharest, Romania

January 28, 2021

## Abstract

A new interpretation on the wobbling structure in  $^{163}\text{Lu}$  is developed, based on the concept of parity symmetry. It is known that four wobbling bands are experimentally observed in this isotope, where three of them are considered as wobbling phonon excitations (namely  $TSD_2$ ,  $TSD_3$ , and  $TSD_4$ ) and the yrast band for the ground state (that is  $TSD_1$ ). In the present work, the trial function that is used for obtaining the wobbling spectrum is analyzed in terms of its behavior under the rotation operation. Indeed, due to a specific symmetry to rotations with  $\pi$  around the 2-axis of the triaxial system, the parity becomes a good quantum number. As such, the trial function admits solutions with negative parity, which belong to the rotational states in  $TSD_4$ . A unified description of all the triaxial super-deformed bands in  $^{163}\text{Lu}$  is achieved with the new formalism.

## 1 Introduction

Triaxiality in nuclei has become an interesting topic for physicists over the years, mainly due to its great challenge of measure it experimentally, but also for its large number of characteristics that are said to be resulting from these kind of shapes. Moreover, stable triaxial shapes are of rare occurrence across the chart of nuclides [1], since the predominant character of nuclei is either spherical or axially symmetric. Over the last two decades, it has been shown that triaxiality plays a crucial role in measurements of important quantities like proton emission probabilities [2], separation energies of the nucleons [1], and also fission barriers in heavy nuclei [3], however, concrete evidences

---

\*E-mail: robert.poenaru@drd.unibuc.ro

†E-mail: raduta@nipne.ro

of triaxiality in nuclei were still missing or under investigation. A tremendous work was given in finding a clear signature for non-axially symmetric shapes: effects such as anomalous signature splitting [4], signature inversion [5], and staggering of  $\gamma$  bands [6] were pointed, but only recently two clear fingerprints of nuclear triaxiality have emerged in the literature, based on both experimental and theoretical findings. Indeed, the phenomena of *chiral symmetry breaking* and that of *wobbling motion* (W.M.) are considered as unique characteristics of nuclear triaxiality.

Chirality consists in the existence of a pair of chiral twin bands with an identical structure and almost similar energies. These bands are expected to appear due to the coupling of valence nucleons and the collective mode of rotation that could drive the total spin away from any of the three principal planes, giving rise to both left-handed and right-handed orientation of the angular momentum vectors [7]. A rigorous investigation of all the nuclei with chiral bands is given by Xiong and Wang in [8], where reportedly a total of 59 chiral doublet bands in 47 such nuclei are confirmed. As a matter of fact, 8 of these nuclei have multiple chiral doublets.

On the other hand, the experimental observations regarding wobbling motion have been quite rare, even though this kind of collective motion has been theoretically predicted almost 50 years ago by Bohr and Mottelson [9] when they were investigating the rotational modes of a triaxial nucleus by means of a Triaxial Rotor Model (TRM). Therein, they showed that for a triaxial rotor, the main rotational motion is around the axis with the largest moment of inertia (MOI), as it is energetically the most favorable. This mode is quantum mechanically disturbed by the rotation around the other two axes, since rotation around any of the three principal axes of the system are possible, due to the anisotropy of the three different MOIs (that is  $\mathcal{I}_1 \neq \mathcal{I}_2 \neq \mathcal{I}_3$ ).

W.M. can be viewed as the quantum analogue to the motion of the asymmetric top, whose rotation around the axis with largest MOI is energetically favored and stable. A uniform rotation about this axis will have the lowest energy for a given angular momentum (spin). As the energy increases, this axis will start to precess with a harmonic type of oscillation about the space-fixed angular momentum vector, giving rise to a family of wobbling bands, each characterized by a wobbling phonon number  $n_w$ . The resulting quantal spectrum will be a sequence of rotational  $\Delta I = 2$  bands, with alternating signature number for each wobbling excitation. According to [9], it is possible to obtain the wobbling spectrum of any triaxial rigid rotor, by using the information related to its angular momentum  $I$ , moments of inertia  $\mathcal{I}_{1,2,3}$ , rotational frequency  $\omega_{\text{rot}}$ , wobbling frequency  $\omega_{\text{wob}}$  as follows:

$$E_{\text{rot}} = \sum_i \left( \frac{\hbar^2}{2\mathcal{I}_i} \right) I_i^2 \approx \frac{\hbar^2}{2\mathcal{I}_1} I(I+1) + \hbar\omega_{\text{wob}} \left( n_w + \frac{1}{2} \right), \quad (1)$$

with  $\omega_{\text{wob}}$  given by the following expression:

$$\hbar\omega_{\text{wob}} = \hbar\omega_{\text{rot}} \sqrt{\frac{(\mathcal{I}_1 - \mathcal{I}_2)(\mathcal{I}_1 - \mathcal{I}_3)}{\mathcal{I}_2\mathcal{I}_3}}, \quad (2)$$

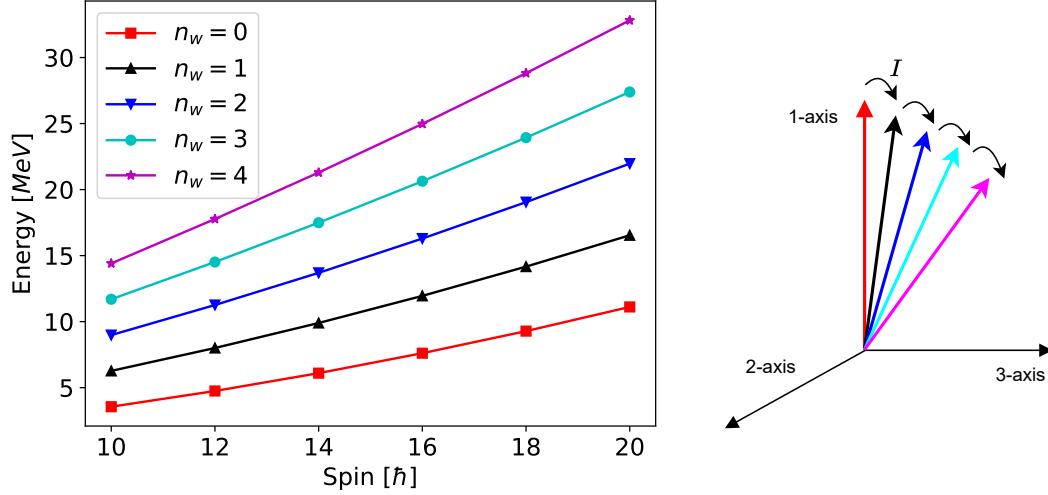


Figure 1: Family of wobbling bands for a simple triaxial rotor (left-side). Tilting of the angular momentum vector away from the rotational axis (right-side). This schematic representation was done for an arbitrary set of MOIs  $\mathcal{I}_1 : \mathcal{I}_2 : \mathcal{I}_3 = 25 : 5 : 2$ .

where the rotational frequency of the rigid rotor is given by  $\hbar\omega_{\text{rot}} = \frac{\hbar I^2}{\mathcal{I}_1}$ . In Eq. 1, the approximation of very large MOI along 1-axis is considered (i.e.,  $\mathcal{I}_1 \gg \mathcal{I}_2, \mathcal{I}_3$ ), and  $I(I+1) = \mathcal{I}_1^2 + \mathcal{I}_2^2 + \mathcal{I}_3^2$ . One can see that the wobbling motion is expressed as a 1-dimensional vibration with only one variable, since the energy of the zero-point fluctuation is  $\frac{\hbar\omega_{\text{wob}}}{2}$  [10].

Just for an illustrative purpose, Figure 1 shows a theoretical spectrum for the wobbling bands within a triaxial rigid rotor. The family of wobbling bands are obtained from a set of three moments of inertia (along the three principal axes), a given angular momentum, and different wobbling phonon numbers. Moreover, in Figure 1, the tilting of the angular momentum away from the rotational axis is sketched, where the tilt increases with the increase in the wobbling excitation. In a given sequence of wobbling bands, both the intra-band  $\Delta I = 2$  as well as inter-band  $\Delta I = 1$  transitions have a strong  $E2$  collective character.

It is important to mention that the wobbling spectrum described by Eq. 1 and graphically represented in Figure 1 was firstly predicted for an even-even triaxial nucleus [9]. This predicted wobbling mode has not been experimentally confirmed yet. However, the first experimental evidence for wobbling excitations in nuclei was for an even-odd nucleus, namely  $^{163}\text{Lu}$ , where a single one-phonon wobbling band was measured initially [11], followed by two additional wobbling bands discovered one year later [12, 13].

After the first discovery of wobbling bands in  $^{163}\text{Lu}$  ( $Z = 71$ ), an entire series of even-odd isotopes with  $A \approx 160$  were experimentally confirmed as *wobblers*:  $^{161}\text{Lu}$ ,  $^{165}\text{Lu}$ ,  $^{167}\text{Lu}$ , and  $^{167}\text{Ta}$ . In these nuclei, the wobbling mode appears due to the coupling of a valence nucleon (the so-called  $\pi(i_{13/2})$  intruder) to a triaxial core, driving the entire nuclear system up to large deformation ( $\epsilon \approx 0.4$ ) [14].

With time, several nuclei in which WM occurs were also reported in regions of smaller  $A$ . Indeed, two isotopes with  $A \approx 130$ :  $^{133}\text{La}$  [15] and  $^{135}\text{Pr}$  [16, 17] were identified as having wobbling bands, which emerged from the coupling with a triaxial even-even core of another intruder (the  $\pi(h_{11/2})$  nucleon) for  $^{135}\text{Pr}$ , and an additional pair of positive parity quasi-protons which are making an alignment with the short axis of the triaxial rotor for  $^{105}\text{Pr}$ . The resulting coupling in both cases have a deformation  $\epsilon = 0.16$  [15, 16], which is obviously smaller than the deformation in the heavier nuclei within the  $A \approx 160$  region. A third nucleus that also lies in this mass region was confirmed very recently by Chakraborty et. al. in [18], namely the odd- $A$   $^{127}\text{Xe}$ , where a total of four wobbling bands have been reported by the team (two yrast bands, and two excited phonon bands with  $n_w = 1$  and  $n_w = 2$ ).

Some additional progress towards a more comprehensive wobbling spectroscopy was made in the  $A \approx 100$  mass region, with an experimental evidence for  $^{105}\text{Pd}$  that showed of two such bands that are built on a  $\nu(h_{11/2})$  configuration, the first one so far in which a valence neutron couples to the triaxial core [19]. The resulting configuration drives the nuclear system up to deformation  $\epsilon \approx 0.26$ .

The heaviest nuclei known so far in which WM has been experimentally observed are the isotopes  $Z = 79$  with  $A = 183$  [20] and  $A = 187$  [21], respectively. However, for the case of  $^{187}\text{Au}$ , there is an ongoing investigation [22] whether the two wobbling bands ( $n_w = 0$  and  $n_w = 1$ ) are bands with wobbling character, or if they are of magnetic nature (which would exclude the wobbling phonon interpretation).

Regarding the wobbling motion for the even-even nuclei (behavior that was described above through the schematic representation from Figure 1), the experimental results are very fragmentary, with unclear evidence on such collective behavior in nuclei. However, some embryos of even-even wobblers have been reported in the recent years. For example, the  $^{112}\text{Ru}$  ( $Z = 44$ ) nucleus has three wobbling bands [23], with two of them being excited (one- and two-phonon wobbling bands). Another example is the even-even  $^{130}\text{Ba}$  ( $Z = 56$ ) [24–26]. Indeed, for  $^{112}\text{Ru}$ , the ground band together with the odd and even spin members of the  $\gamma$  band with were interpreted as zero-(yrast), one-, and two-phonon wobbling bands. Unfortunately, since there are no data concerning the electromagnetic transitions, its wobbling character is still unclear. On the other hand, for the nucleus  $^{130}\text{Ba}$ , from its recent study regarding the band structure [24], a pair of bands with even and odd spins were proposed as zero- and one-phonon wobbling bands, respectively. What it is worth noting for this case is the fact that these two bands are built on a configuration in which two aligned protons that emerge from the bottom of  $h_{j=11/2}$  shell couple with the triaxial core. One remarks the change in nature of the wobbling motion from a purely collective form, but in the presence of two aligned quasiparticles [25].

Regarding the interpretation of the wobbling motion which occurs in the nuclei that were mentioned above, it is mandatory to discuss some aspects related to its behavior with the increase in total angular momentum (nuclear spin). It is a long lasting debate on whether certain nuclei behave as *longitudinal wobblers* (LW) or *transverse wobblers* (TW). The concepts of LW and TW emerged from an extensive study done by Frauendorf et. al. [27] in which the team discussed the possible coupling schemes that a valence

nucleon can create with the triaxial core, thus giving rise to two possible scenarios. Based on microscopic calculations using the Quasiparticle Triaxial Rotor (QTR) model, they showed that if the odd valance nucleon aligns its angular momentum vector  $\vec{j}$  with the axis of largest MOI, the nuclear system is of longitudinal wobbling character. On the other hand, if the odd nucleon aligns its a.m. vector  $\vec{j}$  with an axis perpendicular to the one with largest MOI, then the nuclear system has a transverse wobbling character. From the microscopic calculations, it was shown that for LW, the wobbling energy  $E_{\text{wob}}$  (see Eq. 3) has an *increasing* behavior with an increase in spin, while for TW the energy  $E_{\text{wob}}$  *decreases* with spin.

Within the nuclei that were mentioned above, most of them are of TW type, with only  $^{133}\text{La}$  [15],  $^{127}\text{Xe}$  [18], and  $^{183,187}\text{Au}$  [20, 21] being nuclei with LW character. The energy that characterizes the type of wobbling in a nuclear system is the energy of the first excited band (the one-phonon  $n_w = 1$  wobbling band) relative to the yrast ground band (zero-phonon  $n_w = 0$  wobbling band):

$$E_{\text{wob}} = E_1(I) - \left( \frac{E_0(I+1) + E_0(I-1)}{2} \right), \quad (3)$$

with 0 and 1 representing the wobbling phonon number  $n_w$ .

The odd nucleons that couple with the rigid triaxial core will influence the appearance of a particular wobbling regime (LW or TW). In all the wobblers, there is a proton from a certain orbital which is coupling with the core, except for the case of  $^{105}\text{Pd}$ , where the valence nucleon is a neutron. The nature of the odd quasiparticle (i.e., particle or hole) and its "position" in the deformed  $j$ -shell (i.e. bottom or top) will determine whether its angular momentum  $\vec{j}$  will align with the *short* ( $s$ ) or *long* ( $l$ ) axes of the triaxial rotor, respectively (with the notations short  $s$ , long  $l$ , and medium  $m$  axes of a triaxial ellipsoid). The reasoning behind this has to do with the minimization of the overall energy of the system: in the first case, a maximal overlap of its density distribution with the triaxial core will determine a minimal energy, while in the second case, a minimal overlap of the density distribution of the particle with the core will result in a minimal energy. Moreover, if the quasiparticle emerges from the middle of the  $j$ -shell, then it tends to align its angular momentum vector  $\vec{j}$  with the *medium* ( $m$ ) axis of the triaxial core. Figure 2 aims at depicting the type of alignment of a quasiparticle with the triaxial core.

As previously mentioned, for a given angular momentum, uniform rotation around the axis with the largest MOI corresponds to a minimum energy. For a triaxial rotor, this is equivalent to rotation around the  $m$  axis. Therefore, Frauendorf [27] classified the LW as the situation when the odd nucleon will align its angular momentum along the  $m$ -axis, while TW being the situation where  $j$  is aligned perpendicular to the  $m$ -axis (with  $s$ - or  $l$ -axis alignment depending on the  $j$ -shell orbital from which the odd nucleon arises). It is worthwhile to mention the fact that the analysis done in Ref. [27] was within a so-called *Frozen Alignment* approximation, where the angular momentum of the odd particle  $\vec{j}$  is rigidly aligned with one of the three principal axes of the triaxial ellipsoid (that is  $s$ -,  $l$ - or  $m$ -axis).

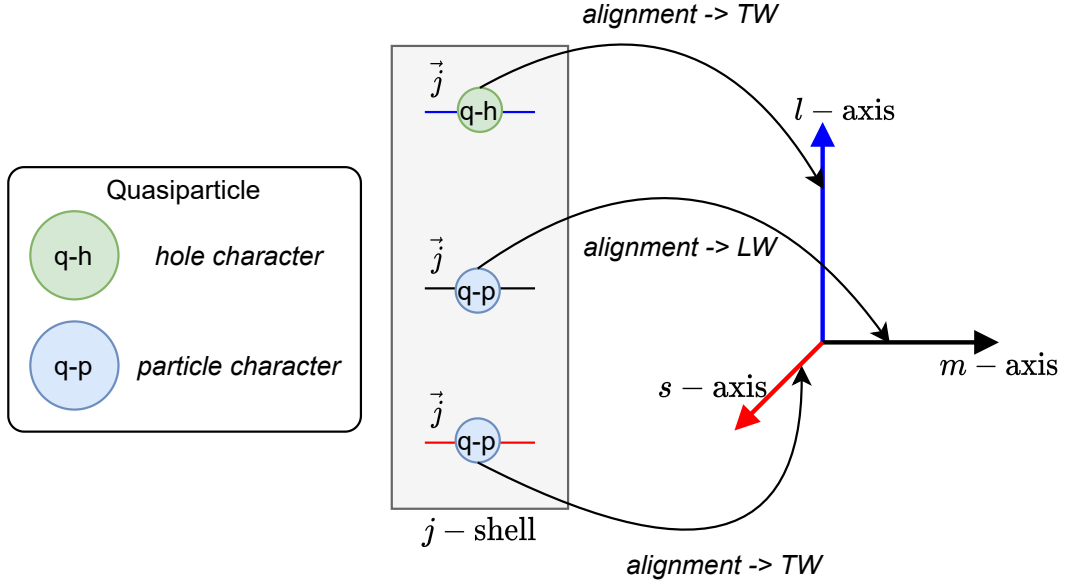


Figure 2: The wobbling regime (LW or TW) based on the type of alignment for an odd quasiparticle with the triaxial core. Figure based on the quantal analysis done in [27].

For a better understanding of the wobbling regimes in terms of angular momentum alignment, the schematic illustration from Figure 3 depicts three particular cases, namely a simple wobbler (the case firstly developed by Bohr and Mottelson [9]) - shown in inset A.0, a longitudinal wobbler - shown in inset A.1, and lastly a transverse wobbler - shown in inset A.1.

In terms of its theoretical analysis, the wobbling motion has been studied using multiple models and interpretations. The Triaxial Particle Rotor Model has been widely used over the recent years [9, 27–30], these being quantal models that can be exactly solved in the laboratory frame. TRM was however, firstly introduced for the motion of a rotating nuclear system by Davydov and Filippov in [31], where they obtained a complete quantal description for the motion of a triaxial nucleus (considering the fact that the nucleus must have a well-defined potential minimum at a non-zero value for the triaxiality parameter  $\gamma$ ). Starting from the framework of Cranking Mean Field Theory (CMFT), there were attempts at extending the cranking model for the study of WM. however, using the mean field approximations, CMFT only help at describing the yrast sequence for a given configuration. In order to improve that, the framework was extended with proper quantum correlations by incorporating the Random Phase Approximation (RPA) theory (see Refs. [32–39] for more details). The method of Collective Hamiltonian [40, 41] was used for the investigation of wobbling spectra in nuclei with the help of deformed potentials which were calculated from the Tilted Axis Cranking (TAC) model. TAC single  $j$ -shell model is also used for the description of the chiral vibrations and rotational motion in deformed nuclei [42, 43]. Mean field approxima-

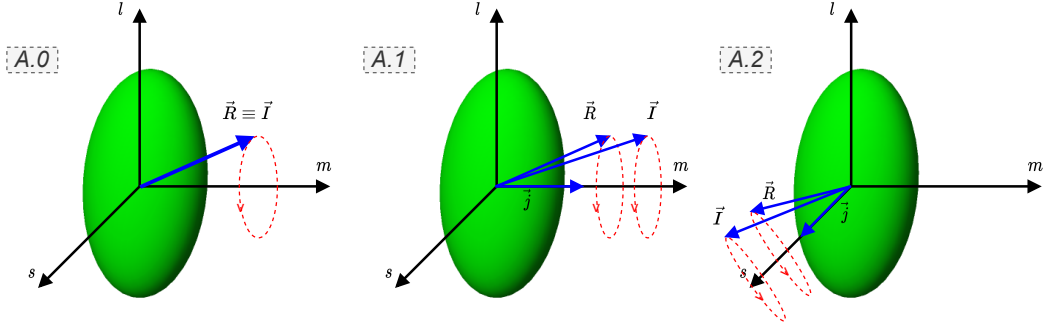


Figure 3: The geometry for the angular momentum for a simple wobbler: A.0, a longitudinal wobbler: A.1, and a transverse wobbler: A.2. The short, long, and medium axes are defined in the body-fixed frame. The vectors  $\vec{R}$ ,  $\vec{j}$ , and  $\vec{I}$  represent the set of angular momenta of the core, odd particle, and the total nuclear system, respectively.

tions were also developed by the so-called *generator coordinate method after angular momentum projection* (GCM+AMP for short), with calculations that emerged from intrinsic cranking states [44]. Some analytical solutions were also developed (based on certain approximations), such as the harmonic approximation (HA) [9, 27, 40, 45], Dyson boson expansion [45, 46], and Holstein-Primakoff (HP) formula [29, 45–48]. The angular momentum projections were also incorporated into the mean field framework, with the recent development of a completely microscopic description of the wobbling motion by Shimada et. al. [49]. A Projected Shell Model (PSM) [50] which starts from the shell-model configuration mixing that is based on a Nilsson deformed mean field was also used for the theoretical study concerning WM. There are alternative developments based on the PSM approach, based on Density Functional Theories (DFT) that can be both non-relativistic [51] as well as relativistic [52].

Other tools that proved to be very efficient for the analysis of the wobbling nuclei are the semi-classical approaches, through which one can obtain equations of motion that describe the nuclear system quite well, starting from quantal Hamiltonians and further applying some de-quantization procedures. The semi-classical approach applied to generalized rotor Hamiltonians has the *advantage* of keeping close contact with the classical picture embedded in the dynamic of the systems. Recently, there has been quite an impressive progress towards realistic description of the wobbling motion [27, 45, 53–57]. As a matter of fact, the present team was able to describe (with a very good agreement) the experimental data concerning the wobbling energies and electromagnetic (e.m.) transition probabilities for the Lu isotopes with  $A = 161, 163, 165, 167$  (see the work done in Refs. [45, 54]), and more recently the odd- $A$   $^{135}\text{Pr}$  isotope [46]. Indeed, starting from a quantal Hamiltonian specific to a triaxial rotor model (that is a triaxial core coupled with an odd valence nucleon) and applying the Time Dependent Variational Equation (TDVE), with a trial function that was carefully chosen, the complete wobbling spectrum of the mentioned isotopes was reproduced, together with the e.m. (intra-band and inter-band) transitions.

Concluding this section, the importance of nuclear triaxiality and the challenges of identifying it experimentally were contoured in the beginning, serving as the starting point of the current work. Furthermore, all the known nuclei in which wobbling motion appears were mentioned (with important observation for some of them). Additionally, the mechanism behind the simple wobblers (the one developed by Bohr and Mottelson [9]) was sketched (starting with Eq. 1), and a family of wobbling bands were schematically represented for a given set MOIs associated to the triaxial rotor (see Figure 1). Lastly, a brief overview with most of the theoretical *tools* that were/are used for describing this elusive phenomenon was realized. Having this in mind, one can say that a detailed outlook for the topic of wobbling motion was properly shown.

Going further, the remaining structure of this current work must be pointed out. In Section 2, an overview with regards to the team's reinterpretation of the wobbling band structure in  $^{163}\text{Lu}$  will be illustrated. This will be the *core-idea* that serves as foundation of this newly developed model. The theoretical formalisms and analytical formulas will be properly presented in Section 3. Experimental results concerning the wobbling spectrum of this isotope will be compared with the newly obtained data in Section 4. Overall conclusions and discussions are reserved to Section 5.

## 2 Re-interpretation of the wobbling bands structure for $^{163}\text{Lu}$

Now that a complete overview of the recent experimental and theoretical results regarding wobbling motion has been made, together with the description of its two regimes (namely, longitudinal wobbling and transverse wobbling), it is worth mentioning the latest progress made by the present team towards the actual interpretation of the wobbling structure of  $^{163}\text{Lu}$ . Considered the *best wobbler* to date,  $^{163}\text{Lu}$  has a rich wobbling spectrum [11,12], with no less than four such wobbling bands: one yrast -  $TSD_1$ , which has a zero-phonon wobbling number  $n_w = 0$ ), and three excited wobbling bands -  $TSD_{2,3,4}$  with their corresponding wobbling phonon numbers  $n_w = 1, 2, 3$ , respectively. The name TSD comes from Triaxial Strongly Deformed bands. The triaxial bands emerge due to the coupling of an odd- $\vec{j}$  nucleon with an even-even triaxial core. Thus, for  $^{163}\text{Lu}$ , it is the intruder  $\pi(i_{13/2})$  that couples to the triaxial core [11,13,28], driving the nuclear system up to large deformation, and stabilizing the deformed structure. Indeed, a triaxial shape with deformation parameters  $(\epsilon_2, \gamma) \approx (0.38, +20^\circ)$  is assumed to be in agreement with the observed data, based on calculations using the Ultimate Cranker Code [58] for the potential energy surface (PES).

In terms of experimental evidence which should be pointing out wobbling nature for the four TSD bands belonging to  $^{163}\text{Lu}$ , the large transition quadrupole moment  $Q_t \approx 10\text{ b}$  [59] (which is substantially larger than it is the case for normal-deformed bands), the predominantly  $E2$  character of the transitions linking adjacent bands ( $I \rightarrow I - 1$ ), a large  $E2/M1$  mixing ratio  $\delta > 1$  for the transitions linking the yrare ( $n_w = 1$ ) and yrast ( $n_w = 0$ ) bands (which obviously should result in smaller transitions with magnetic character, or in other words, there is no  $M1$  dominance) are clear fingerprints



of wobbling nature. For a set of results concerning these quantities (both theoretical and experimental), see Ref. [45], and the references cited therein. Another quantity that indicate strong deformation with wobbling character is the relative rigid rotor energy, and for this isotope calculations show that all four bands have a similar behavior with respect to this value (see Figures 3 and 4 from Ref. [60]).

Considering the experimental evidence which was indicated above and calculations based on particle rotor models, it can be summarized that the *generally accepted* formalism for the band structure in  $^{163}\text{Lu}$  is the following:

- There are three excited wobbling bands (w.b.):  $TSD_2$ ,  $TSD_3$ , and  $TSD_4$ .
- The three excited w.b. have wobbling-phonon numbers  $n_{w_2} = 1$ ,  $n_{w_3} = 2$ , and  $n_{w_4} = 3$ , respectively.
- All three bands are built on top of the yrast state (the ground state band) with zero-wobbling-phonon number  $n_{w_1} = 0$ .
- Stable triaxial super-deformation is achieved due to the alignment of the odd  $\pi(i_{13/2})$  nucleon which couples to a triaxially deformed core  $\vec{R}$ .
- $TSD_{1,2,3}$  have all positive parity  $\pi_1 = \pi_2 = \pi_3 = +1$ , while the spin states belonging to  $TSD_4$  have negative parity  $\pi_4 = -1$ . All states within the four bands have half-integer spin, obviously.

In accordance with the band structure which was just formulated, a full description of the wobbling spectrum of  $^{163}\text{Lu}$  was done within a semi-classical formalism by Raduta et. al. [45]. Therein, with the TDVE applied on the PRM Hamiltonian with a trial wave-function that encapsulates both the states of the deformed nucleus  $I$  and the single-particle states  $j$ , a set of analytical expressions for the excitation energies of all four bands was obtained. The energies belonging to the excited wobbling phonons were populated by the action of a phonon operator  $\Gamma^\dagger$  on the ground state. Indeed, by acting with the operator one on the ground state with the spin  $I = R + j$  and  $R = 0, 2, 4, \dots$ , the states from  $TSD_2$  ( $n_w = 1$ ) can be obtained. By applying twice ( $n_w = 2$ ) the phonon operator, the rotational states from  $TSD_3$  will be created. Lastly, the states from  $TSD_4$  are obtained with the action on the ground state with three ( $n_w = 3$ ) phonon operators: two of positive parity and one of negative parity (due to the overall negative parity  $\pi_4 = -1$  of  $TSD_4$ ). One has to remark the fact that for  $TSD_4$ , the model assumes an odd-particle-rotor with a different intruder: the  $\pi(h_{9/2})$  nucleon. This was suggested by the negative parity orbital which might be occupied by this proton, in the spherical shell model. Several calculations in the literature point out that this nucleon might be causing the third excited wobbling band to have negative parity [61]. It is worthwhile mentioning that for the work described in [45], the variational principle was only applied for the states in  $TSD_1$ , since the other three wobbling bands are obtained through phononic excitations with the corresponding operator.

In what follows, it is useful to introduce some notations that will refer to the formalisms developed by the team in describing the wobbling motion in  $^{163}\text{Lu}$ . As such,

the work developed in [56, 57] will be denoted to W1, while the current work (which is in fact an extension of W1) will be shortly denoted by W2. For the sake of a self-consistent presentation, in the following subsection 2.1 a brief overview of the recently published work W1 will be made, with further development that has W1 as a starting ground being presented in the second subsection 2.2 - representing the *core concept* of the current team's investigation.

## 2.1 W1 - Signature Partner Bands

Working with a semi-classical approach that is based on the triaxial particle rotor model, a full description of the wobbling bands for  $^{163}\text{Lu}$  was achieved, but with a slightly modified band structure. Indeed, rather than applying a TDVE just for the yrast  $TSD_1$  band, the states from  $TSD_2$  were also obtained variationally. This was possible due to the different coupling schemes that emerged for  $TSD_1$  and  $TSD_2$ , respectively. More precisely, in [57] and [56] there are three different coupling schemes ( $\vec{R} + \vec{j}$ ): states from  $TSD_1$  arise from the odd  $\pi(i_{13/2})$  intruder coupling with a core with angular momentum sequence  $R_1 = 0, 2, 4, \dots$ ; states from  $TSD_2$  arise from the same odd proton but coupling with a different triaxial core with angular momentum sequence  $R_2 = 1, 3, 5, \dots$ . The band  $TSD_3$  is obtained as a set of states which are built on top of  $TSD_2$ , with the action of a wobbling frequency with wobbling phonon number  $n_w = 1$ ; this being different than the band structure previously mentioned where the third band was a two-phonon excitation of the yrast  $TSD_1$ . Lastly, the fourth band  $TSD_4$  is a ground state band which results from the coupling of the same core as for  $TSD_2$  (that is defined with the angular momentum sequence  $R_2 = 1, 3, 5, \dots$ ) but with a different odd nucleon:  $\pi(h_{9/2})$ . Consequently,  $TSD_2$  and  $TSD_4$  are yrast states, alongside  $TSD_1$ . Each band represents a collection of energy levels describing ground states that correspond to distinct sets of angular momenta.

For the first three bands, the MOIs are the same, and they are considered to be free parameters within the numerical calculations. However, this is not true for the fourth band, where a different set of MOIs had to be introduced, since for  $TSD_4$  the core polarization effects are changed by coupling scheme.

Using W1, the final results pointed out to a largest MOI corresponding to the 1-axis (with  $\mathcal{I}_1$  being the largest MOI obtained through the fitting procedure), making the system rotate around the 1-axis (that is the short axis). Moreover, the odd proton is aligned to the short axis as well, suggesting that the nucleus has a LW character. By representing the experimental wobbling energies according to Eq. 3, it was obtained that both theoretical as well as the experimental values were increasing functions with respect to an increase in angular momentum (keep in mind that the first wobbling band  $n_w = 1$  within the W1 model is  $TSD_3$ ). The agreement between the two sets of data (see Figure 6 from [56]) indicate that the condition for LW/TW character of the wobbling bands stated by Frauendorf et. al. in [27] is not strictly related to the increasing/decreasing wobbling energy  $E_{\text{wob}}$ . In fact, Guo et. al. [22] also point out that the approximation of Frozen Alignment (FA) from [27] neglects the Coriolis interaction of the single particle. There is an ongoing debate whether the behavior of an LW or TW triaxial nucleus is

strictly related to the change in  $E_{wob}$  with total a.m. [62–64].

A final aspect that needs to be mentioned regarding W1 has to do with the interpretation of  $TSD_1$  and  $TSD_2$  as being Signature Partner Bands (SPB). Signature [9] is a quantum property which appears in deformed systems. It is strictly related to the invariance of a system with quadrupole deformation (its nuclear wave-function) to a rotation by an angle  $\pi$  around a principal axis. For example, a rotation around the  $x$ -axis will be defined as an operator:

$$\hat{R}_x = e^{i\pi\hat{I}_x} . \quad (4)$$

As for the framework used in [56, 57], due to the wave-function describing the system being written as a product between the  $|I\rangle$  basis state corresponding to the total angular momentum and the single-particle basis state  $|j\rangle$ , the rotation operator used in W1 achieves the following form:

$$\hat{R}_x(\pi) = e^{-i\pi\hat{I}_x} \otimes e^{-i\pi\hat{j}_x} . \quad (5)$$

If the system has an axial symmetry, only the rotation around any of the principal axes that are perpendicular to the symmetry one can define the signature quantum number. Consequently, signature is a property specific to a deformed system and it translates to a so-called *deformation invariance* with respect to the space and time reflection properties [9]. For an even-even nucleus, the signature operator  $\hat{R}_x$  has two eigenvalues, -1 and 1. For the even-odd case, the eigenvalues are  $-i$  and  $+i$ , and depending on its total spin, the signatures can have to values, given by the following assignment:

$$\alpha_I = \frac{1}{2} (-1)^{I-1/2} . \quad (6)$$

Indeed, Eq. 6 describes the signature quantum number for a state of angular momentum  $I$  belonging to an odd mass nucleus. Such a rotational band with a sequence of states differing in spin by  $\Delta I = 1$  will be divided into two branches, each branch consisting of levels differing in spin by  $\Delta I = 2$ , being related by the signature number  $\alpha_I = \pm 1/2$ . In [56] the signature concept is brought to the classical picture associated to a triaxial nucleus by means of rotation operators which act on the trial function (this function is a product of two coherent states, one that is associated to the core and one to the valence nucleon). Eqs. 27-29 from [56] will extract two signatures for  $TSD_1$  and  $TSD_2$ , namely the *favoured* signature  $\alpha_{1f} = +1/2$  for the first band, and *un-favoured* signature  $\alpha_{2u} = -1/2$  for the second band, respectively. A justification for the possibility of  $TSD_1$  and  $TSD_2$  of being SPB was based on the calculation of the triaxial potential (which was systematically performed in [45] and [54]), concluding that the minimum is very deep, preventing in this way the states from  $TSD_2$  to share other minima through tunneling effects. Other experimental and theoretical results [65–68] for deformed nuclei around this mass region suggest that the calculations performed in W1 regarding the connection between  $TSD_1$  and  $TSD_2$  as belonging to a signature splitting phenomenon are valid and consistent with already existing interpretations.

It is instructive to mention a few key-points which arise based on the above discussion regarding W1 can be summarized as follows:

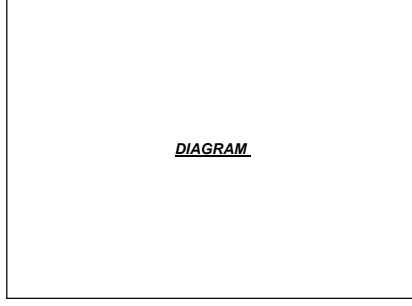


Figure 4: The general workflow involving W1 model.

- (a) The wobbling band structure in  $^{163}\text{Lu}$  was re-interpreted: three bands are now yrast ground states, and only  $TSD_3$  is one-phonon excited wobbling band (built on top of  $TSD_2$ )
- (b) Both  $TSD_1$  and  $TSD_2$  are obtained variationally, by solving the time dependent variational equation associated to the initial quantal Hamiltonian
- (c) There are three different  $R + j$  coupling schemes that will produce the entire spectra:
  - (i) Coupling  $C_1$ : The odd proton  $j_1 = 13/2$  is coupled to a core sequence with a.m.  $R_1 = 0, 2, 4, \dots$  (even spin states for the triaxial rotor).
  - (ii) Coupling  $C_2$ : The same odd proton  $j_1 = 13/2$  as in  $C_1$  is coupled to a core sequence with a.m.  $R_2 = 1, 3, 5, \dots$  (odd spin states for the triaxial rotor).
  - (iii) Coupling  $C_3$ : A different odd proton  $j_2 = 9/2$  is coupled to the same core as in  $C_2$ .
- (d) Two different sets of MOIs corresponding to the triaxial nucleus (that is the rotor coupled with the odd proton) are obtained as fitting parameters throughout the numerical calculations: one for the set  $TSD_{1,2,3}$  and one for  $TSD_4$ .
- (e)  $TSD_1$  and  $TSD_2$  are Signature Partner Bands: with  $TSD_1$  ( $TSD_2$ ) being the favored (un-favored) partner. Their corresponding signature quantum numbers are  $\alpha_{1f} = +1/2$  and  $\alpha_{2u} = -1/2$ .
- (f) As a side-by-side comparison with regards to the overall agreement with the experimental data, W1 yielded better results than compared to the previous work depicted in Ref. [53], although it must be mentioned that both models are based on semi-classical approaches.

A diagram which shows the workflow involved in W1 can be seen in the Figure 4. Also, a comparison with previous calculations can be seen in Figure 21 from Ref. [56].

## 2.2 W2 - Signature Partner Bands + Parity Partner Bands

The main question which can be asked regarding the formalism W1 that was described in 2.1 is whether it is possible to obtain a *unified* description for all four bands in  $^{163}\text{Lu}$  in relation to the coupling scheme. In other words, it is worth investigating the possibility of having a unique single-particle state  $j$  that is coupled to a core of positive parity for the bands  $TSD_{1,2,3}$  and a core of negative parity for  $TSD_4$ .

Fortunately, the answer is positive: starting from the semi-classical formalism of W1, one can properly adjust the coupling scheme, making sure that the entire numerical recipe used for obtaining the energy spectrum of  $^{163}\text{Lu}$  remains consistent with the experimental results.

Regarding the unique single-particle that couples to the triaxial core, it is natural to pick the  $i_{13/2}$  proton (that is  $j_1$  from W1). Reasoning behind this choice has to do with the microscopic calculations [10, 13, 61] that showed stable triaxial structures in the  $^{163}\text{Lu}$  potential energy surface when the triaxial core couples with a highly aligned  $j$ -shell particle, strongly indicating the  $\pi(i_{13/2})$  proton. Keep in mind that a highly aligned  $j$ -nucleon will *prefer* to keep a certain triaxial deformation when coupled to a core [69–71] (in the sense that the triaxiality parameter  $\gamma$  will have a certain value based on the orbital of the odd nucleon), and using microscopic calculations following the Ultimate Cranker code, it has been shown that a value of  $\gamma \approx +20^\circ$  is preferred by the odd  $\pi(i_{13/2})$  nucleon.

By taking  $j_1$  as the sole intruder that couples to a positive core and also a negative core, the sequences with even/odd integer spins for the core do not change. In fact, the coupling schemes can be readily obtained, making sure that the final (experimental) spin sequences for each TSD band is intact.

- (a) Coupling  $C'_1$ : the odd  $j_1$  proton aligns with the core of even-integer spin sequence  $R_1 = 0, 2, 4, \dots$ , with a parity of the  $R_1$  core that is positive  $\pi(R_1) = +1$ .
- (b) Coupling  $C'_2$ : the odd  $j_1$  proton aligns with the core of even-integer spin sequence  $R_2^+ = 1, 3, 5, \dots$ , with a parity of the  $R_2^+$  core that is positive  $\pi(R_2^+) = +1$ .
- (c) Coupling  $C'_3$ : the odd  $j_1$  proton aligns with the core with an odd-integer spin sequence  $R_2^- = 1, 3, 5, \dots$ , which has negative parity  $\pi(R_2^-) = -1$ .

From the three schemes defined above, it is clear that  $C'_1$  corresponds to the yrast  $TSD_1$ ,  $C'_2$  to the ground state  $TSD_2$ , and finally  $C'_3$  to the ground state  $TSD_4$ . Obviously, the odd valence nucleon  $j_1$  has a positive parity  $\pi_{j_1} = +1$ . There has not been attributed a coupling scheme for  $TSD_3$ , since this band still remains as the one-wobbling phonon excitation that is built on top of  $TSD_2$  with the action of a phonon operator which will be characterized later on. The three couplings are schematically represented in Figure 5.

It is expected that the Hamiltonian of the system will keep a similar form, since there are no new interactions or modified particle-core states added in the problem. The argument holds because the coupling scheme which involves the fourth triaxial band

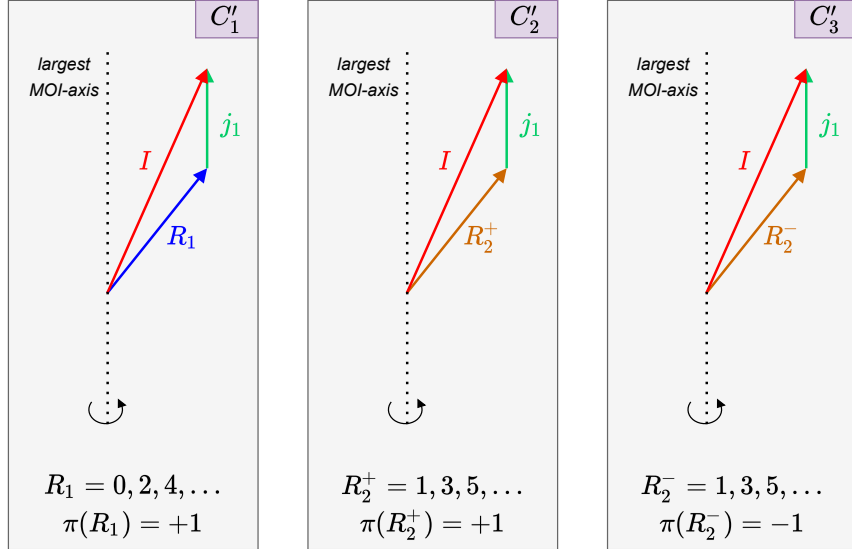


Figure 5: A schematic representation with the three coupling schemes that characterize the W2 model. The same odd particle (the  $j_1 = i_{13/2}$  proton) is coupling with two positive cores with even/odd integer spin sequences for  $TSD_1/TSD_2$ , and one negative core in the case of  $TSD_4$ . The total spin of the system precesses around the axis with the largest MOI, as it is the case for a triaxial rotor.

$TSD_4$  only the single-particle's angular momentum state changes, but the core has negative parity. As a result, the treatment of the problem will follow the same manner as it did in the W1 case.

The last step in searching for a unified coupling scheme in  $^{163}\text{Lu}$  is to establish a possible relationships between the four bands. As per the calculations involved in W1, it was proven that signature quantum number is a good quantum number and indeed, a sign that  $TSD_1$  and  $TSD_2$  are signature partners emerged. Their overall similar properties and spin difference enforce this argument. Furthermore, in this new W2 approach, the difference in parity between the  $TSD_2$  and  $TSD_4$  but the same angular momentum sequence of their corresponding triaxial core  $R_2^+$  and  $R_2^-$  strongly suggest that the two bands are *Parity Partner Bands*: two rotational sequences with energy states characterized by opposite parity, increasing energy that follows a trend  $\propto I(I+1)$ , and a spin difference  $\Delta I = 2$  between states belonging to the same band. In the following section, calculations which will show that parity is indeed a good quantum number for the triaxial rotor + odd-particle system will be provided. For what it is worth mentioning now is that the concept of parity partners between  $TSD_2$  and  $TSD_4$  emerge from the idea that a stable strongly deformed structure is achieved from a single quasiparticle which moves in a quadrupole mean-field generated by a triaxial even-even core. However, there is a splitting in two different cases of coupling mechanisms, namely  $C'_2/C'_3$  depending on the alignment of the high- $j$ -shell particle with a core of positive/negative parity.

Similar structures with alternating positive-negative parity bands have been also re-

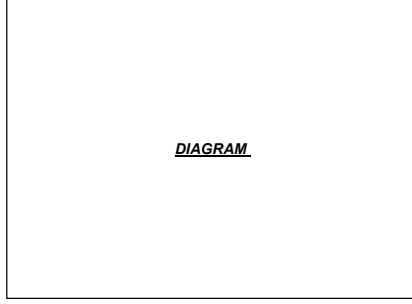


Figure 6: The general workflow involving W2 model.

ported in other nuclei such as  $^{40}\text{Ca}$  [72], or some heavier isotopes like  $^{218}\text{Fr}$  [73]. In fact, one of the authors of this present work developed a unified description of states with positive and negative parity in odd-mass nuclei [74, 75], although therein, a quadrupole-octupole term was introduced within the particle-core Hamiltonian to describe this feature. Concluding the current subsection, a diagram which shows the workflow involved in W2 can be seen in the Figure 6.

### 3 Theoretical Background

In this section, a description of the framework used for obtaining the wobbling spectrum of  $^{163}\text{Lu}$  is made. As stated in the previous section, the system is described with a similar Hamiltonian used in W1, namely the Hamiltonian for a triaxial PRM model.

$$H = H_{\text{core}} + H_{\text{s.p.}} . \quad (7)$$

The Hamiltonian in Eq. 7 describes a system in which an odd  $j$  quasiparticle interacts with a triaxial even-even core, where the odd nucleon is moving in a quadrupole deformed mean field that is generated by the core itself. As such, the first  $H_{\text{core}}$  term in the Hamiltonian corresponds describes the motion triaxial core, while the second term  $H_{\text{s.p.}}$  represents the aligned valence proton ( $j_1$  in this case).

Indeed, the core Hamiltonian is given by:

$$H_{\text{core}} = \sum_{i=1,2,3} \frac{1}{2\mathcal{I}_i} (I_i - j_i)^2 , \quad (8)$$

where the core angular momentum is  $\vec{R} = \vec{I} - \vec{j}$  and the terms  $\mathcal{I}_i$  represent the moments of inertia for triaxial ellipsoid along the principal axes. These three moments of inertia will be considered as free parameters in the present calculations, but, compared to the work W1, a unique set of MOIs will be attributed to the four bands, since the triaxial core will create an alignment with a unique single particle, that is  $j_1$ . Because of this, there is not option for their nature (i.e., rigid or hydrodynamic).

The single-particle Hamiltonian from Eq. 7 is derived from the well-known Nilsson potential [76, 77]:

$$h(\beta_2, \gamma) = C \left\{ \cos \gamma Y_{20}(\theta, \varphi) + \frac{\sin \gamma}{\sqrt{2}} [Y_{22}(\theta, \varphi) + Y_{2-2}(\theta, \varphi)] \right\} , \quad (9)$$

where the coupling parameter  $C$  causes the level splitting in the deformed field and it is directly proportional to the quadrupole deformation  $\beta_2$ . The potential  $h$  from Eq. 9 is written in terms of the quadrupole deformation and triaxiality parameter that play the role of deformation parameters within a triaxial system  $(\beta_2, \gamma)$ . Its expression using the coupling parameter  $C$  is widely used when working with a particle-rotor-model [78–80]. In our case, by applying a Wigner-Eckart theorem for the single- $j$  particle, the following expression for  $H_{\text{s.p.}}$  will be obtained:

$$H_{\text{s.p.}} = \frac{V}{j(j+1)} \left[ \cos \gamma (3j_3^2 - \vec{j}^2) - \sqrt{3} \sin \gamma (j_1^2 - j_2^2) \right] + \epsilon_j . \quad (10)$$

This term describes the motion of an odd particle with angular momentum  $j$  in a mean field generated by a triaxial core, with a potential strength  $V$  characterized by the quadrupole deformation ( $V \propto \beta_2$ ). In fact, the single-particle potential strength  $V$  will be considered as fourth free parameter within the calculations and its behavior will dictate the coupling of the  $j_1$  particle with all four TSD bands. The term  $\epsilon_j$  from Eq. 10 represents the single particle energy that corresponds to the odd  $j_1$  proton from the  $i$ -orbital.

Regarding the triaxial deformation  $\gamma$  which enters in Eq. 10, its value will be considered as another free parameter of the current problem. In other words, having  $V$  and  $\gamma$  as free parameters means that the system will be described by its deformation parameters which will be obtained through a fitting procedure, keeping an agreement with the experimental data regarding the excitation energies of the rotational states belonging to  $TSD_{1,2,3,4}$ .

From Eqs. 8 and 10, the free parameter set can be obtained, hereafter denoted by  $\mathcal{P}$ . It comprises three moments of inertia, the single particle potential strength, and the triaxial deformation. As such,  $\mathcal{P}$  can be written as:

$$\mathcal{P} = [\mathcal{I}_1, \mathcal{I}_2, \mathcal{I}_3, V, \gamma] . \quad (11)$$

Solving the problem of W2 is equivalent to finding the eigenvalues of  $H$  given in Eq. 7. In a similar approach as in W1, the eigenvalues of interest are obtained on the base of a semi-classical approach. Thus, the first step is to perform a de-quantization procedure on  $H$  through a TDVE [45, 53, 55]:

$$\delta \int_0^t \langle \Psi_{IjM} | H - i \frac{\partial}{\partial t'} | \Psi_{IjM} \rangle dt' = 0 . \quad (12)$$

Working within a semi-classical approach allows one to keep a close contact with the system's dynamics in terms of *friendly* and *familiar* equations of motion and generalized



coordinates. The trial function from Eq. 12 is carefully chosen as a product of two basis states comprising the states with total angular momentum  $I$  and  $j$ , respectively:

$$|\Psi_{IjM}\rangle = \mathbf{N} e^{z\hat{I}_-} e^{s\hat{j}_-} |IMI\rangle |jj\rangle , \quad (13)$$

where the operators  $\hat{I}_-$  and  $\hat{j}_-$  denote the lowering operators for the intrinsic angular momenta  $\vec{I}$  and  $\vec{j}$ , respectively, and  $\mathbf{N}$  plays the role of the normalization constant. One must remark the fact that the states from Eq. 13 are extremal states for the operators  $(\hat{I}^2, \hat{I}_3)$  and  $(\hat{j}^2, \hat{j}_3)$ , respectively, and they correspond to the maximally allowed states for a given set of angular momenta  $I$  and  $j$ . As an observation, the trial function is an admixture of components of definite  $K$ , which is consistent with the fact that for a triaxial nucleus,  $K$  is not a good quantum number.

The variables  $z$  and  $s$  from Eq. 13 are complex functions that depend on time, and they play the role of classical coordinates of the phase spaces that describe the motion of the core and the odd particle:

$$z = \rho e^{i\varphi} , \quad s = f e^{i\psi} . \quad (14)$$

In order to obtain a set of classical equations which describe the motion of the system, a new pair of variables are introduced from the ones defined in Eq. 14. Indeed, defining the variables  $(\varphi, r)$  and  $(\psi, t)$  with  $r$  and  $t$  given by the relations:

$$r = \frac{2I}{1 + \rho^2} , \quad t = \frac{2j}{1 + f^2} , \quad (15)$$

where  $r \in [0, 2I]$  and  $t \in [0, 2j]$ , will bring the classical equations of motion (provided by the TDVE), to a straightforward canonical form:

$$\begin{aligned} \frac{\partial \mathcal{H}}{\partial r} &= \dot{\varphi} ; \quad \frac{\partial \mathcal{H}}{\partial \varphi} = -\dot{r} , \\ \frac{\partial \mathcal{H}}{\partial t} &= \dot{\psi} ; \quad \frac{\partial \mathcal{H}}{\partial \psi} = -\dot{t} . \end{aligned} \quad (16)$$

The function  $\mathcal{H}$  denotes the average of the Hamiltonian operator  $H$  (Eq. 7) with the trial function  $|\Psi_{IjM}\rangle$  given in Eq. 13, and it plays the role of classical energy. It represents a crucial quantity within the present analysis, at it will provide an insight with regards to the stability of the wobbling motion in  $^{163}\text{Lu}$ , and can help to pinpoint several regions where the wobbling mode is stable/unstable. This analysis will be performed in the following sections.

$$\mathcal{H} \equiv \mathcal{H}(\bar{q}_{\text{core}}; \bar{q}_{\text{s.p.}}) = \langle \Psi_{IjM} | H | \Psi_{IjM} \rangle , \quad (17)$$

where the set of coordinates  $(\varphi, r)$  and  $(\psi, t)$  were conveniently denoted with  $\bar{q}_{\text{core}}$  and  $\bar{q}_{\text{s.p.}}$ , respectively, since they describe the motion of the core and that of the odd single-particle.

Starting from the equations of motion given in Eq. 16, one can observe that the function  $\mathcal{H}$  is a constant of motion, that is  $\dot{\mathcal{H}} \equiv 0$ . This equation will define a surface,

a so-called equi-energy surface  $\mathcal{H} = \text{const.}$  It is worth mentioning the fact that such an equality holds since the entire set of equations of motion emerged from a variational principle. The sign of the Hessian associated to this classical function will indicate its stationary points. Among them, some are minima. One such example of minimum points for  $\mathcal{H}$  is the point  $p_0 \equiv (q_{\text{core}}; q_{\text{s.p.}})|_{\text{min}} = (\varphi, r; \psi, t)|_{\text{min}} = (0, I; 0, j)$ . The energy function is minimum  $\mathcal{H}_{\text{min}}^{(I,j)} = H(p_0)$  as long as the condition on the MOIs is:  $\mathcal{I}_1 > \mathcal{I}_2 > \mathcal{I}_3$ . There is no restriction on  $\gamma$ .

With a linearization procedure for the equations of motion around the minimum point  $p_0$  of  $\mathcal{H}$ , a dispersion equation will be obtained:

$$\Omega^4 + B\Omega^2 + C = 0 . \quad (18)$$

The above equation describes a harmonic type of motion for the nuclear system, with the solutions to this algebraic equation as the *wobbling frequencies*  $\Omega$ . The terms  $B$  and  $C$  are complex functions of total angular momentum  $I$ , single particle a.m.  $j$ , inertial parameters  $A_k = 1/(2\mathcal{I}_k)$ ,  $k = 1, 2, 3$ , single particle potential strength  $V$ , and triaxiality parameter  $\gamma$ . In fact, one can conclude that  $B$  and  $C$  are functions which depend on the parameter set defined in Eq. 11:  $B = f_B(\mathcal{P}, I, j)$  and  $C = f_C(\mathcal{P}, I, j)$ , respectively.

$$-B = [(2I - 1)(A_3 - A_1) + 2jA_1] [(2I - 1)(A_2 - A_1) + 2jA_1] + 8A_2A_3Ij + (\mathbf{T}_B^1 \times \mathbf{T}_B^2) , \quad (19)$$

where the terms  $\mathbf{T}_B^1$  and  $\mathbf{T}_B^2$  are defined defined as:

$$\begin{aligned} \mathbf{T}_B^1 &= \left[ (2j - 1)(A_3 - A_1) + 2IA_1 + V \frac{2j - 1}{j(j + 1)} \sqrt{3}(\sqrt{3} \cos \gamma + \sin \gamma) \right] , \\ \mathbf{T}_B^2 &= \left[ (2j - 1)(A_2 - A_1) + 2IA_1 + V \frac{2j - 1}{j(j + 1)} 2\sqrt{3} \sin \gamma \right] . \end{aligned} \quad (20)$$

$$\begin{aligned} C &= \{ [(2I - 1)(A_3 - A_1) + 2jA_1] \times \mathbf{T}_C^1 - 4IjA_3^2 \} \times \\ &\times \{ [(2I - 1)(A_2 - A_1) + 2jA_1] \times \mathbf{T}_C^2 - 4IjA_2^2 \} , \end{aligned} \quad (21)$$

where the terms  $\mathbf{T}_C^1$  and  $\mathbf{T}_C^2$  are defined defined as:

$$\begin{aligned} \mathbf{T}_C^1 &= \left[ (2j - 1)(A_3 - A_1) + 2IA_1 + V \frac{2j - 1}{j(j + 1)} \sqrt{3}(\sqrt{3} \cos \gamma + \sin \gamma) \right] , \\ \mathbf{T}_C^2 &= \left[ (2j - 1)(A_2 - A_1) + 2IA_1 + V \frac{2j - 1}{j(j + 1)} 2\sqrt{3} \sin \gamma \right] . \end{aligned} \quad (22)$$

It can be seen that the terms which enter in  $B$  and  $C$ , namely  $(\mathbf{T}_B^1, \mathbf{T}_B^2)$  from Eq. 20 and  $(\mathbf{T}_C^1, \mathbf{T}_C^2)$  from Eq. 22 that enter in  $B$  and  $C$  correspond to the quadrupole

deformation that causes the single particle to move in the mean-field of the triaxial core. The terms also define the triaxiality that the nucleus achieves once the odd proton couples to the triaxial core, driving the system up to a large (and stable) deformation.

Going back to Eq. 18, under the restrictions for the MOIs defined above, the dispersion equation admits two real and positive solutions (hereafter denoted with  $\Omega_1^I$  and  $\Omega_2^I$ , where  $\Omega_1^I < \Omega_2^I$ ) defined for  $j_1 = i_{13/2}$ , given by:

$$\Omega_{1,2}^I = \sqrt{\frac{1}{2} (-B \mp (B^2 - 4C)^{1/2})} . \quad (23)$$

These two solutions are interpreted as *wobbling frequencies* associated to the motion of the core, and the motion of the odd-particle. As such, each wobbling frequency has an associated wobbling-phonon number:

$$\Omega_1^I \rightarrow n_{w_1} ; \Omega_2^I \rightarrow n_{w_2} . \quad (24)$$

It is worth noting that they take part in the energy states belonging to all the bands, including the yrast ones, however, in that case, the zero-point motion is considered (meaning that the two wobbling quanta ( $\Omega_1^I, \Omega_2^I$ ) are halved).

Now that the energy function  $\mathcal{H}$  was defined in terms of classical coordinates  $\bar{q}_{\text{core}}$  and  $\bar{q}_{\text{s.p.}}$ , and the wobbling frequencies were obtained, it is possible to define the analytical expressions for the four TSD bands of  $^{163}\text{Lu}$ . Indeed, taking care of the coupling scheme for each band, they can be formulated as follows:

$$\begin{aligned} E_{\text{TSD1}}^I &= \epsilon_j + \mathcal{H}_{\text{min}}^{(I,j)} + \mathcal{F}_{00}^I , \quad I = 13/2, 17/2, 21/2 \dots \\ E_{\text{TSD2}}^I &= \epsilon_j^1 + \mathcal{H}_{\text{min}}^{(I,j)} + \mathcal{F}_{00}^I , \quad I = 27/2, 31/2, 35/2 \dots \\ E_{\text{TSD3}}^I &= \epsilon_j + \mathcal{H}_{\text{min}}^{(I-1,j)} + \mathcal{F}_{10}^I , \quad I = 33/2, 37/2, 41/2 \dots \\ E_{\text{TSD4}}^I &= \epsilon_j^2 + \mathcal{H}_{\text{min}}^{(I,j)} + \mathcal{F}_{00}^I , \quad I = 47/2, 51/2, 55/2 \dots , \end{aligned} \quad (25)$$

where  $\mathcal{F}_{n_{w_1} n_{w_2}}^I$  is a function of the wobbling frequencies, defined accordingly to the wobbling phonon numbers  $n_{w_1}, n_{w_2}$ :

$$\mathcal{F}_{n_{w_1} n_{w_2}}^I = \Omega_1^I \left( n_{w_1} + \frac{1}{2} \right) + \Omega_2^I \left( n_{w_2} + \frac{1}{2} \right) , \quad (26)$$

and  $\mathcal{H}_{\text{min}}^{(I,j)}$  is the classical energy evaluated in its minimal point  $p_0$ .

A few aspects regarding the energy spectrum defined in Eq. 25 are worth mentioning. To each band there is a specific energy  $\epsilon_j$  associated to the single-particle state from the orbital that it belongs to. In this case, the odd-proton  $j_1$  with  $j = 13/2$  from the  $i$ -orbital is the one that couples to the triaxial core. However, for the bands  $\text{TSD}_2$  and  $\text{TSD}_4$ , a different re-normalization is considered, since the former is the unfavored partner within the structure, and the latter is the negative parity partner within the band structure. These quantities will shift the overall energy states belonging to the two bands, each by a different amount. As a result, both  $\epsilon_j^1$  and  $\epsilon_j^2$  will be adjusted throughout the

| Band    | $n_{w_1}$ | $n_{w_2}$ | $\pi$ | $\alpha$ | Coupling scheme  |
|---------|-----------|-----------|-------|----------|------------------|
| $TSD_1$ | 0         | 0         | +1    | +1/2     | $C'_1$           |
| $TSD_2$ | 0         | 0         | +1    | -1/2     | $C'_2$           |
| $TSD_3$ | 1         | 0         | +1    | +1/2     | Built on $TSD_2$ |
| $TSD_4$ | 0         | 0         | -1    | -1/2     | $C'_3$           |

Table 1: The wobbling phonon numbers, parities, signatures, and coupling schemes assigned to each triaxial band in  $^{163}\text{Lu}$ , within the W2 model. The three coupling schemes were defined in Section 2.2.

the numerical calculations such that the energy spectrum is best reproduced. Another aspect concerns the band  $TSD_3$ ; since this is the only excited wobbling band within the family, its configuration is built on top of  $TSD_2$ , with the action of a single phonon ( $n_{w_1} = 0$ ) operator, that is the wobbling frequency  $\Omega_1^I$ . Consequently, an energy state  $I$  belonging to  $TSD_3$  is obtained from a state  $I - 1$  from  $TSD_2$ . In Table 1, the rest of the wobbling phonon numbers are mentioned, with the parity, signature, and coupling scheme for each band in particular.

### 3.1 Parity quantum number for the wave-function

In W1 it was shown that signature emerges from the calculations on the total wave-function as a good quantum number for this triaxial system. This is why in [56] the bands  $TSD_1$  and  $TSD_2$  appeared as Signature Partner Bands (SPB). In W2, this property still stands.

Since the backbone of the current work started from the need for a single odd-particle that couples to a triaxial core in  $^{163}\text{Lu}$ , one has to look at the band  $TSD_4$  (which was interpreted as having a different nucleon:  $j_2$  with  $j = 9/2$  from the  $h$ -orbital), and see if its differentiating properties can be linked to *main group* of bands (namely  $TSD_{1,2,3}$ ). Indeed, from the experimental measurements regarding spin and parity assignment [61], it turns out that the parity of the rotational states are negative. Therefore, a forensic analysis on this quantum property should be considered as the necessary ingredient in a unified description of all four bands.

Choosing the rotation axis as the 2-axis, one can define the parity operator as a product of the complex conjugation operation and a rotation of angle  $\pi$  around this axis:  $P = e^{-i\pi\hat{I}_2}C$ . Obviously,  $\hat{I}_2$  represents the rotation operator and  $C$  the operator performs a complex conjugation when applied on a wave-function. The total parity operator is defined as the product of an operator corresponding to the core and one corresponding to the single particle:

$$\mathcal{P}_T = P_{\text{core}}P_{\text{s.p.}} . \quad (27)$$

Acting with the total parity operator defined above, on the trial function  $\Psi(\bar{q}_{\text{core}}; \bar{q}_{\text{s.p.}})$  associated to the triaxial system (which was defined in Eq. 13), the following is obtained:

$$\mathcal{P}_T\Psi(r, \varphi; t, \psi) = \Psi(r, \varphi + \pi; t, \psi + \pi) \stackrel{\text{not.}}{=} \bar{\Psi}. \quad (28)$$

Keep in mind that the set of classical phase space which describe the individual dynamics of the core and the single-particle, namely  $\bar{q}_{\text{core}}$  and  $\bar{q}_{\text{s,p}}$ , were defined as  $(r, \varphi)$  and  $(t, \psi)$ .

The classical energy function  $\mathcal{H}$  has an invariance property at changing the angles with  $\pi$ :

$$\mathcal{H}(r, \varphi; t, \psi) = \mathcal{H}(r, \varphi + \pi; t, \psi + \pi) . \quad (29)$$

From Eqs. 28 and 29, it can be concluded that the wave-function describing the triaxial system  $\Psi$  and its image through  $\mathcal{P}_T$ ,  $\bar{\Psi}$ , are two linearly dependent functions which differ only by a multiplicative constant  $\mu$ , with  $|\mu| = 1$ . Thus,  $\mu$  can either be -1 or +1, such that:

$$\Psi(r, \varphi + \pi; t, \psi + \pi) = \pm \Psi(r, \varphi; t, \psi) . \quad (30)$$

The above result concludes the parity analysis for the wave-function, showing that the triaxial rotor admits eigenfunctions (i.e., deformed rotational states) of negative parity. Therefore, a single wave-function characterized by the coupling of a triaxial core to the odd proton  $i_{13/2}$  is describing both positive parity states ( $\in TSD_{1,2,3}$ ) as well as negative parity states ( $\in TSD_4$ ). This analysis, together with the fact that  $TSD_2$  and  $TSD_4$  have the same a.m. sequences (although  $TSD_2$  has more states with low spin than  $TSD_4$ ) suggest the fact that these two bands might be Parity Partners.

### 3.2 Energy function - geometrical interpretation

The analytical expression for the average of  $H$  with the trial function describing the system was previously calculated in W1. Indeed, the energy function  $\mathcal{H}$  was given in terms of the phase space coordinates as follows:

$$\begin{aligned} \mathcal{H} = & \frac{I}{2}(A_1 + A_2) + A_3 I^2 + \frac{2I-1}{2I} r(2I-r) \mathcal{A}_\varphi + \frac{j}{2}(A_1 + A_2) + A_3 j^2 + \frac{2j-1}{2j} t(2j-t) \mathcal{A}_\psi \\ & - 2\sqrt{r(2I-r)t(2j-t)} \mathcal{A}_{\varphi\psi} + A_3 [r(2j-t) + t(2I-r)] - 2A_3 Ij + V \frac{2j-1}{j+1} \mathcal{A}_\gamma , \end{aligned} \quad (31)$$

with:

$$\begin{aligned} \mathcal{A}_\varphi &= (A_1 \cos^2 \varphi + A_2 \sin^2 \varphi - A_3) , \\ \mathcal{A}_{\varphi\psi} &= (A_1 \cos \varphi \cos \psi + A_2 \sin \varphi \sin \psi) , \\ \mathcal{A}_\psi &= (A_1 \cos^2 \psi + A_2 \sin^2 \psi - A_3) , \\ \mathcal{A}_\gamma &= \left[ \cos \gamma - \frac{t(2j-t)}{2j^2} \sqrt{3} (\sqrt{3} \cos \gamma + \sin \gamma \cos 2\psi) \right] \end{aligned} \quad (32)$$

It is instructive to check the dependence of the energy function on the angular momentum components, e.g. the coordinates  $x_k \stackrel{\text{not.}}{=} I_k$ ,  $k = 1, 2, 3$ , where the quantization

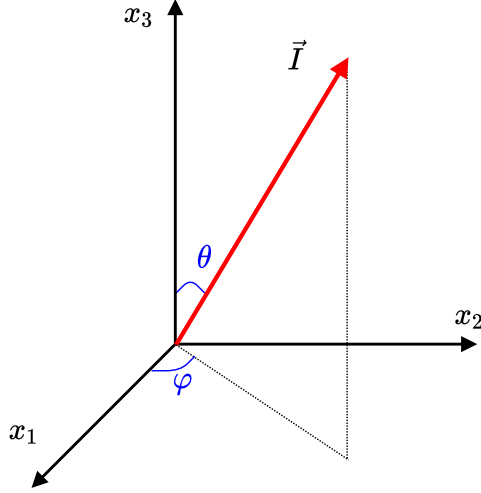


Figure 7: The angular momentum vector of the triaxial nucleus, represented in the angular momentum space. The polar angles  $(\theta, \varphi)$  that the vector makes with the  $x_3$  axis and  $x_1x_2$ -plane, respectively, are also shown.

axis is chosen as the 3-axis. By expressing the angular momentum coordinates  $x_{1,2,3}$  in terms of the polar angles  $(\theta, \varphi)$  and a radius  $r$  given by the value of the total angular momentum  $I$ , one obtains:

$$x_1 = I \sin \theta \cos \varphi, \quad x_2 = I \sin \theta \sin \varphi, \quad x_3 = I \cos \theta. \quad (33)$$

The total angular momentum  $\vec{I}$  of the nucleus can be visualized as a vector within the angular momentum space, generated by its three components. Figure 7 shows such a representation.

Within this spherical coordinates, and evaluating the energy function around its minimum point  $p_0$ , the following expression for  $\mathcal{H}$  arises:

$$\mathcal{H} |_{p_0} = I \left( I - \frac{1}{2} \right) \sin^2 \theta (A_1 \cos^2 \varphi + A_2 \sin^2 \varphi - A_3) - 2A_1 I j \sin \theta + T_{\text{core}} + T_{\text{s.p.}}. \quad (34)$$

The last two terms in this equation are independent on the polar angles  $(\theta, \varphi)$ , and they characterize the minimal energy for a triaxial rotor with given spin  $I$  and inertial parameters  $A_{1,2,3}$  (i.e.,  $T_{\text{core}}$ ), and the minimal energy which arises from the coupling  $j$  nucleon that is moving in the mean-field of strength  $V$  and triaxial deformation  $\gamma$  (i.e.,  $T_{\text{s.p.}}$ ). The two terms have the following form:

$$\begin{aligned} T_{\text{core}} &= \frac{I}{2} (A_1 + A_2) + A_3 I^2, \\ T_{\text{s.p.}} &= \frac{j}{2} (A_2 + A_3) + A_1 j^2 - V \frac{2j-1}{j+1} \sin \left( \gamma + \frac{\pi}{6} \right). \end{aligned} \quad (35)$$

The classical equation of motion admits two constants of motion: the total system energy ( $E$ ) and the total angular momentum ( $I$ ). In fact, this is consistent with the quantum theory, where the angular momentum vector of a rotating system is conserved. A 3-dimensional rotation can be visualized in a semi-classical description as a precession of the total angular momentum vector around the rotational axis (that is the axis with largest MOI). Consequently, by finding the intersection line(s) between the surface of the energy ellipsoid  $E$  and the surface of the angular momentum sphere generated by the spin  $I$ , then one can assert that a trajectory which belongs to a defined rotational state (with given spin and energy) is found. It is possible to construct a set with all the allowed trajectories for  $^{163}\text{Lu}$  if the energy ellipsoid  $E$  for a given state  $I \in TSD_k$ ,  $k = 1, 2, 3, 4$  is evaluated, then intersected with its corresponding angular momentum  $I$ . Such representations will be made in the following section. These trajectories will show aim to show a classical visualization of the wobbling character for a triaxial nucleus.

## 4 Numerical results

### References

- [1] Peter Möller, Ragnar Bengtsson, B Gillis Carlsson, Peter Olivius, and Takatoshi Ichikawa. Global calculations of ground-state axial shape asymmetry of nuclei. *Physical review letters*, 97(16):162502, 2006.
- [2] DS Delion, RJ Liotta, and Ramon Wyss. Theories of proton emission. *Physics reports*, 424(3):113–174, 2006.
- [3] Peter Möller, Arnold J Sierk, Takatoshi Ichikawa, Akira Iwamoto, Ragnar Bengtsson, Henrik Uhrenholt, and Sven Åberg. Heavy-element fission barriers. *Physical Review C*, 79(6):064304, 2009.
- [4] I Hamamoto and H Sagawa. Triaxial deformation in odd- $z$  light rare-earth nuclei. *Physics Letters B*, 201(4):415–419, 1988.
- [5] R Bengtsson, H Frisk, FR May, and JA Pinston. Signature inversion—a fingerprint of triaxiality. *Nuclear Physics A*, 415(2):189–214, 1984.
- [6] J Stachel, N Kaffrell, E Grosse, H Emling, H Folger, R Kulesa, and D Schwalm. Triaxiality and its dynamics in  $^{104}\text{Ru}$  investigated by multiple coulomb excitation. *Nuclear Physics A*, 383(3):429–467, 1982.
- [7] Stefan Frauendorf and Jie Meng. Tilted rotation of triaxial nuclei. *Nuclear Physics A*, 617(2):131–147, 1997.
- [8] BW Xiong and YY Wang. Nuclear chiral doublet bands data tables. *Atomic Data and Nuclear Data Tables*, 125:193–225, 2019.

- [9] Aage Bohr and Ben R Mottelson. *Nuclear structure*, volume 1. World Scientific, 1998.
- [10] Gudrun B Hagemann and Ikuko Hamamoto. Quantized wobbling in nuclei. *Nuclear Physics News*, 13(3):20–24, 2003.
- [11] SW Ødegård, GB Hagemann, DR Jensen, M Bergström, B Herskind, G Sletten, S Törmänen, JN Wilson, PO Tjøm, I Hamamoto, et al. Evidence for the wobbling mode in nuclei. *Physical review letters*, 86(26):5866, 2001.
- [12] DR Jensen, GB Hagemann, I Hamamoto, SW Ødegård, B Herskind, G Sletten, JN Wilson, K Spohr, H Hübel, P Bringel, et al. Evidence for second-phonon nuclear wobbling. *Physical review letters*, 89(14):142503, 2002.
- [13] D Ringkøbing Jensen, GB Hagemann, I Hamamoto, SW Ødegård, M Bergström, B Herskind, G Sletten, S Törmänen, JN Wilson, PO Tjøm, et al. Wobbling phonon excitations, coexisting with normal deformed structures in 163lu. *Nuclear Physics A*, 703(1-2):3–44, 2002.
- [14] H Schnack-Petersen, Ragnar Bengtsson, RA Bark, P Bosetti, A Brockstedt, H Carlsson, LP Ekström, GB Hagemann, B Herskind, F Ingebretsen, et al. Superdeformed triaxial bands in 163,165 lu. *Nuclear Physics A*, 594(2):175–202, 1995.
- [15] S Biswas, R Palit, S Frauendorf, U Garg, W Li, GH Bhat, JA Sheikh, J Sethi, S Saha, Purnima Singh, et al. Longitudinal wobbling in 133 la. *The European Physical Journal A*, 55(9):1–7, 2019.
- [16] James Till Matta. Transverse wobbling in 135 pr. In *Exotic Nuclear Excitations: The Transverse Wobbling Mode in 135 Pr*, pages 77–93. Springer, 2017.
- [17] N Sensharma, U Garg, S Zhu, AD Ayangeakaa, S Frauendorf, W Li, GH Bhat, JA Sheikh, MP Carpenter, QB Chen, et al. Two-phonon wobbling in 135pr. *Physics Letters B*, 792:170–174, 2019.
- [18] S Chakraborty, HP Sharma, SS Tiwary, C Majumder, AK Gupta, P Banerjee, S Ganguly, S Rai, S Kumar, A Kumar, et al. Multiphonon longitudinal wobbling in 127xe. *Physics Letters B*, 811:135854, 2020.
- [19] J Timár, QB Chen, B Kruzsicz, D Sohler, I Kuti, SQ Zhang, J Meng, P Joshi, R Wadsworth, K Starosta, et al. Experimental evidence for transverse wobbling in pd 105. *Physical review letters*, 122(6):062501, 2019.
- [20] S Nandi, G Mukherjee, QB Chen, S Frauendorf, R Banik, Soumik Bhattacharya, Shabir Dar, S Bhattacharyya, C Bhattacharya, S Chatterjee, et al. First observation of multiple transverse wobbling bands of different kinds in au 183. *Physical Review Letters*, 125(13):132501, 2020.



- [21] N Sensharma, U Garg, QB Chen, S Frauendorf, DP Burdette, JL Cozzi, KB Howard, S Zhu, MP Carpenter, P Copp, et al. Longitudinal wobbling motion in  $^{187}\text{Au}$ . *Physical review letters*, 124(5):052501, 2020.
- [22] S Guo, XH Zhou, CM Petrache, EA Lawrie, S Mthembu, YD Fang, HY Wu, HL Wang, HY Meng, GS Li, et al. Risk of misinterpretation of low-spin non-yrast bands as wobbling bands. *arXiv preprint arXiv:2011.14354*, 2020.
- [23] JH Hamilton, SJ Zhu, YX Luo, AV Ramayya, S Frauendorf, JO Rasmussen, JK Hwang, SH Liu, GM Ter-Akopian, AV Daniel, et al. Super deformation to maximum triaxiality in  $a=100-112$ ; superdeformation, chiral bands and wobbling motion. *Nuclear Physics A*, 834(1-4):28c–31c, 2010.
- [24] CM Petrache, PM Walker, S Guo, QB Chen, S Frauendorf, YX Liu, RA Wyss, D Mengoni, YH Qiang, A Astier, et al. Diversity of shapes and rotations in the  $\gamma$ -soft  $^{130}\text{Ba}$  nucleus: First observation of a t-band in the  $a=130$  mass region. *Physics Letters B*, 795:241–247, 2019.
- [25] YK Wang, FQ Chen, and PW Zhao. Two quasiparticle wobbling in the even-even nucleus  $^{130}\text{Ba}$ . *Physics Letters B*, 802:135246, 2020.
- [26] QB Chen, S Frauendorf, and CM Petrache. Transverse wobbling in an even-even nucleus. *Physical Review C*, 100(6):061301, 2019.
- [27] S Frauendorf and F Dönau. Transverse wobbling: A collective mode in odd- $a$  triaxial nuclei. *Physical Review C*, 89(1):014322, 2014.
- [28] Ikuko Hamamoto. Wobbling excitations in odd- $a$  nuclei with high- $j$  aligned particles. *Physical Review C*, 65(4):044305, 2002.
- [29] Kosai Tanabe and Kazuko Sugawara-Tanabe. Algebraic description of triaxially deformed rotational bands in odd mass nuclei. *Physical Review C*, 73(3):034305, 2006.
- [30] Shi Wen-Xian and Chen Qi-Bo. Wobbling geometry in a simple triaxial rotor. *Chinese Physics C*, 39(5):054105, 2015.
- [31] AS Davydov and GF Filippov. Rotational states in even atomic nuclei. *Nuclear Physics*, 8:237–249, 1958.
- [32] Yoshifumi R Shimizu and Masayuki Matsuzaki. Nuclear wobbling motion and electromagnetic transitions. *Nuclear Physics A*, 588(3):559–596, 1995.
- [33] Masayuki Matsuzaki, Yoshifumi R Shimizu, and Kenichi Matsuyanagi. Wobbling motion in atomic nuclei with positive- $\gamma$  shapes. *Physical Review C*, 65(4):041303, 2002.

- [34] Masayuki Matsuzaki, Yoshifumi R Shimizu, and Kenichi Matsuyanagi. Dynamical moments of inertia associated with wobbling motion in the triaxial superdeformed nucleus. *The European Physical Journal A-Hadrons and Nuclei*, 20(1):189–190, 2003.
- [35] Masayuki Matsuzaki and Shin-Ichi Ohtsubo. Instability of nuclear wobbling motion and tilted axis rotation. *Physical Review C*, 69(6):064317, 2004.
- [36] Masayuki Matsuzaki, Yoshifumi R Shimizu, and Kenichi Matsuyanagi. Nuclear moments of inertia and wobbling motions in triaxial superdeformed nuclei. *Physical Review C*, 69(3):034325, 2004.
- [37] Yoshifumi R Shimizu, Masayuki Matsuzaki, and Kenichi Matsuyanagi. High-k precession modes: Axially symmetric limit of wobbling motion in the cranked random-phase approximation description. *Physical Review C*, 72(1):014306, 2005.
- [38] Yoshifumi R Shimizu, Takuya Shoji, and Masayuki Matsuzaki. Parametrizations of triaxial deformation and  $e 2$  transitions of the wobbling band. *Physical Review C*, 77(2):024319, 2008.
- [39] Takuya Shoji and Yoshifumi R Shimizu. Microscopic calculation of the wobbling excitations employing the woods-saxon potential as a nuclear mean-field. *Progress of theoretical physics*, 121(2):319–355, 2009.
- [40] QB Chen, SQ Zhang, PW Zhao, and J Meng. Collective hamiltonian for wobbling modes. *Physical Review C*, 90(4):044306, 2014.
- [41] QB Chen, SQ Zhang, J Meng, et al. Wobbling motion in pr 135 within a collective hamiltonian. *Physical Review C*, 94(5):054308, 2016.
- [42] S Mukhopadhyay, D Alameh, U Garg, S Frauendorf, T Li, PV Madhusudhana Rao, X Wang, SS Ghugre, MP Carpenter, S Gros, et al. From chiral vibration to static chirality in nd 135. *Physical review letters*, 99(17):172501, 2007.
- [43] Bin Qi, SQ Zhang, J Meng, SY Wang, and S Frauendorf. Chirality in odd-a nucleus 135nd in particle rotor model. *Physics Letters B*, 675(2):175–180, 2009.
- [44] Makito Oi, Ahmad Ansari, Takatoshi Horibata, and Naoki Onishi. Wobbling motion in the multi-bands crossing region. *Physics Letters B*, 480(1-2):53–60, 2000.
- [45] AA Raduta, R Poenaru, and L Gr Ixaru. Semiclassical unified description of wobbling motion in even-even and even-odd nuclei. *Physical Review C*, 96(5):054320, 2017.
- [46] AA Raduta, CM Raduta, and R Poenaru. A new boson approach for the wobbling motion in even-odd nuclei. *Journal of Physics G: Nuclear and Particle Physics*, 48(1):015106, 2020.

- [47] K Tanabe and K Sugawara-Tanabe. Triaxiality in nuclear rotational states. *Physics Letters B*, 34(7):575–578, 1971.
- [48] Kosai Tanabe and Kazuko Sugawara-Tanabe. Selection rules for electromagnetic transitions in triaxially deformed odd- $a$  nuclei. *Physical Review C*, 77(6):064318, 2008.
- [49] Mitsuhiro Shimada, Yudai Fujioka, Shingo Tagami, and Yoshifumi R Shimizu. Rotational motion of triaxially deformed nuclei studied by the microscopic angular-momentum-projection method. i. nuclear wobbling motion. *Physical Review C*, 97(2):024318, 2018.
- [50] Kenji Hara and Yang Sun. Projected shell model and high-spin spectroscopy. *International Journal of Modern Physics E*, 4(04):637–785, 1995.
- [51] PW Zhao, P Ring, and J Meng. Configuration interaction in symmetry-conserving covariant density functional theory. *Physical Review C*, 94(4):041301, 2016.
- [52] M Konieczka, Markus Kortelainen, and W Satuła. Gamow-teller response in the configuration space of a density-functional-theory-rooted no-core configuration-interaction model. *Physical Review C*, 97(3):034310, 2018.
- [53] AA Raduta, R Budaca, and CM Raduta. Semiclassical description of a triaxial rigid rotor. *Physical Review C*, 76(6):064309, 2007.
- [54] AA Raduta, R Poenaru, and Al H Raduta. Wobbling motion in  $lu$  within a semi-classical framework. *Journal of Physics G: Nuclear and Particle Physics*, 45(10):105104, 2018.
- [55] R Budaca. Tilted-axis wobbling in odd-mass nuclei. *Physical Review C*, 97(2):024302, 2018.
- [56] AA Raduta, R Poenaru, and CM Raduta. New approach for the wobbling motion in the even-odd isotopes  $lu$  161, 163, 165, 167. *Physical Review C*, 101(1):014302, 2020.
- [57] AA Raduta, R Poenaru, and CM Raduta. Towards a new semi-classical interpretation of the wobbling motion in  $^{163}lu$ . *Journal of Physics G: Nuclear and Particle Physics*, 47(2):025101, 2020.
- [58] Tord Bengtsson. The high-spin structure of  $^{158}er$ : A theoretical study. *Nuclear Physics A*, 512(1):124–148, 1990.
- [59] A Görgen, RM Clark, M Cromaz, P Fallon, GB Hagemann, H Hübel, IY Lee, AO Macchiavelli, G Sletten, D Ward, et al. Quadrupole moments of wobbling excitations in  $lu$  163. *Physical Review C*, 69(3):031301, 2004.
- [60] GB Hagemann. Triaxiality and wobbling. *Acta Physica Polonica B*, 36(4):1043, 2005.

- [61] DR Jensen, GB Hagemann, I Hamamoto, B Herskind, G Sletten, JN Wilson, SW Ødegård, K Spohr, H Hübel, P Bringel, et al. Coexisting wobbling and quasi-particle excitations in the triaxial potential well of 163 Lu. *The European Physical Journal A-Hadrons and Nuclei*, 19(2):173–185, 2004.
- [62] Kosai Tanabe and Kazuko Sugawara-Tanabe. Stability of the wobbling motion in an odd-mass nucleus and the analysis of pr 135. *Physical Review C*, 95(6):064315, 2017.
- [63] S Frauendorf. Comment on “stability of the wobbling motion in an odd-mass nucleus and the analysis of pr 135”. *Physical Review C*, 97(6):069801, 2018.
- [64] Kosai Tanabe and Kazuko Sugawara-Tanabe. Reply to “comment on ‘stability of the wobbling motion in an odd-mass nucleus and the analysis of pr 135’”. *Physical Review C*, 97(6):069802, 2018.
- [65] Yang Sun, Shuxian Wen, et al. Varied signature splitting phenomena in odd proton nuclei. *Physical Review C*, 50(5):2351, 1994.
- [66] AM Khalaf, Hayam Yassin, and Eman R Abo Elyazeed. Properties of signature partner superdeformed bands in mercury nuclei. *Journal: JOURNAL OF ADVANCES IN PHYSICS*, 11(1), 2015.
- [67] VS Uma and Alpana Goel.  $\delta i = 1$  staggering in signature partner pairs of superdeformed rotational bands in the  $a = 190$  mass region. *The European Physical Journal Plus*, 130(6):1–6, 2015.
- [68] HM Mittal and Anshul Dadwal. Signature partner pairs of superdeformed rotational bands in 192Tl. In *Proceedings of the DAE-BRNS Symp. on Nucl. Phys*, volume 61, page 134, 2016.
- [69] Ikuko Hamamoto and Ben Mottelson. On the intrinsic spectra of rotating nuclei with tri-axial shape. *Physics Letters B*, 127(5):281–285, 1983.
- [70] Ikuko Hamamoto. Rotational motion of triaxial shape in unfavoured-signature states of odd- $a$  nuclei. *Physics Letters B*, 193(4):399–404, 1987.
- [71] Ikuko Hamamoto. Interplay between one-particle and collective degrees of freedom in nuclei. *Physica Scripta*, 91(2):023004, 2016.
- [72] S Torilov, S Thummerer, W Von Oertzen, Tz Kokalova, G De Angelis, HG Bohlen, A Tumino, M Axiotis, E Farnea, N Marginean, et al. Spectroscopy of 40 Ca and negative-parity bands. *The European Physical Journal A-Hadrons and Nuclei*, 19(3):307–317, 2004.
- [73] ME Debray, MA Cardona, D Hojman, AJ Kreiner, M Davidson, J Davidson, H Sommacal, G Levinton, DR Napoli, S Lenzi, et al. Alternating parity bands in 87 218 fr. *Physical Review C*, 62(2):024304, 2000.

- [74] AA Radutaa and CM Radutab. The csm extension for the description of positive and negative parity bands in even-odd nuclei. *arXiv preprint arXiv:0903.0076*, 2009.
- [75] AA RADUTA and CM Raduta. Simultaneous description of positive and negative parity bands in even-even and even-odd nuclei. *ANNALS OF THE UNIVERSITY OF CRAIOVA, PHYSICS*, 21(1):28–53, 2011.
- [76] J Meyer-ter Vehn. Collective model description of transitional odd-a nuclei:(i). the triaxial-rotor-plus-particle model. *Nuclear Physics A*, 249(1):111–140, 1975.
- [77] SY Wang, SQ Zhang, B Qi, J Peng, JM Yao, J Meng, et al. Description of  $\pi$  g  $9/2$   $\nu$  h  $11/2$  doublet bands in rh 106. *Physical Review C*, 77(3):034314, 2008.
- [78] J Peng, J Meng, and SQ Zhang. Description of chiral doublets in a 130 nuclei and the possible chiral doublets in a 100 nuclei. *Physical Review C*, 68(4):044324, 2003.
- [79] T Koike, K Starosta, and I Hamamoto. Chiral bands, dynamical spontaneous symmetry breaking, and the selection rule for electromagnetic transitions in the chiral geometry. *Physical review letters*, 93(17):172502, 2004.
- [80] SY Wang, SQ Zhang, B Qi, and J Meng. Doublet bands in cs 126 in the triaxial rotor model coupled with two quasiparticles. *Physical Review C*, 75(2):024309, 2007.